AGU ADVANCING EARTH AND SPACE SCIENCE

JGR Atmospheres

RESEARCH ARTICLE

10.1029/2022JD037296

Key Points:

- Localized maximum incremental reactivities (MIRs) were established for volatile organic compounds (VOCs) in major Chinese metropolitan areas
- Regional average MIRs are well representative of MIRs for most individual cities
- Localized MIRs and US MIRs shared a similar pattern but differed for a few species

Supporting Information:

Supporting Information may be found in the online version of this article.

Correspondence to:

L. Xue,
xuelikun@sdu.edu.cn

Citation:

Zhang, Y., Xue, L., Mu, J., Chen, T., Li, H., Gao, J., & Wang, W. (2022). Developing the maximum incremental reactivity for volatile organic compounds in major cities of Central-Eastern China. *Journal of Geophysical Research: Atmospheres*, *127*, e2022JD037296. https://doi.org/10.1029/2022JD037296

Received 13 JUN 2022
Accepted 4 NOV 2022

Developing the Maximum Incremental Reactivity for Volatile Organic Compounds in Major Cities of Central-Eastern China

Yingnan Zhang[1], Likun Xue[1], Jiangshan Mu[1], Tianshu Chen[1], Hong Li[2], Jian Gao[2], and Wenxing Wang[1,2]

[1]Environment Research Institute, Shandong University, Qingdao, China, [2]Chinese Research Academy of Environmental Sciences, Beijing, China

Abstract The Chinese government has identified volatile organic compounds (VOCs) management as a key priority in the fourteenth Five-Year Plan (2021–2025) to alleviate ground-level ozone (O_3) air pollution. To provide scientific support for VOCs management, we developed the localized maximum incremental reactivity (MIR) for 57 VOCs species (prescribed by the Photochemical Assessment Monitoring Stations (PAMS)) in eight representative cities and averaged urban conditions over Central-Eastern China, with application of the Master Chemical Mechanism box model coupled with solid observational constraints. Though the exact environmental conditions differ among cities, all of them are in VOCs-limited O_3 formation regime, underlining the importance of VOCs to O_3 formation. The MIRs constructed based on regional average scenarios are well representative of those constructed based on individual cities, with Guangzhou as an exception due to its vast variance in chemical environments. The localized MIRs displayed the same overall pattern as the U.S. MIRs, but differed largely with respect to a few species (especially alkenes), owing to a combined influence of many factors. We applied the localized MIRs to quantify the concentration-weighted ozone formation potential (OFP), which elucidate the importance of aromatics to O_3 formation in the Chinese metropolitan areas. The top 10 key VOC species together with their explicitly tracked emission sources were determined, which could offer references for the formulation of effective control policies. The localized MIRs developed in this study can be applied to quantify OFPs for VOCs in Chinese cities, which has a great significance to VOCs management and O_3 pollution control.

Plain Language Summary Tropospheric ozone is a key component of photochemical smog and would adversely affect human health and climate change. The ozone formation in Chinese metropolitan areas is usually limited by volatile organic compounds (VOCs) that include a large variety of species. Evaluating the reactivity of individual VOC species and their effects on ozone formation has been hindered due to the lack of localized Maximum Incremental Reactivity (MIR) values. In this study, we addressed this issue by developing the MIRs based upon a combination of representative Chinese urban conditions and detailed chemical box modeling. We reveal that regional average MIRs are well representative of MIRs for most individual cities via inter-comparison of the localized results in China. In contrast, there is a noneligible difference in MIRs between China and the U.S., owing to influence of the chemical mechanisms and atmospheric environmental conditions. These findings have great significance for VOCs control in China and other countries suffering from serious ozone air pollution.

1. Introduction

Ground-level ozone (O_3) air pollution has emerged as a major environmental concern in China in the recent decade (Lu et al., 2018; Wang et al., 2017, 2022). Since 2013, the Chinese government has taken a series of strict measures to reduce anthropogenic emissions, and the observed decreases in the concentrations of nitrogen oxides ($NO_x = NO + NO_2$; one of the major O_3 precursors) and other routinely monitored pollutants (such as sulfur dioxide, carbon monoxide, and particulate matters) demonstrate the great success of air pollution control (Liu & Wang, 2020b; Zheng et al., 2018). However, the ambient O_3 concentrations exhibited significant upward trends as evidenced by multiyear observations in a number of studies (Sun et al., 2016; Wang et al., 2019, 2022; Xu, 2021; Xu et al., 2020). The persistently worsening O_3 pollution stimulated the Chinese government and atmospheric chemists to devote more efforts on another type of major O_3 precursors, that is, volatile organic compounds (VOCs), the control of which is still largely lagged in China (Li et al., 2019).

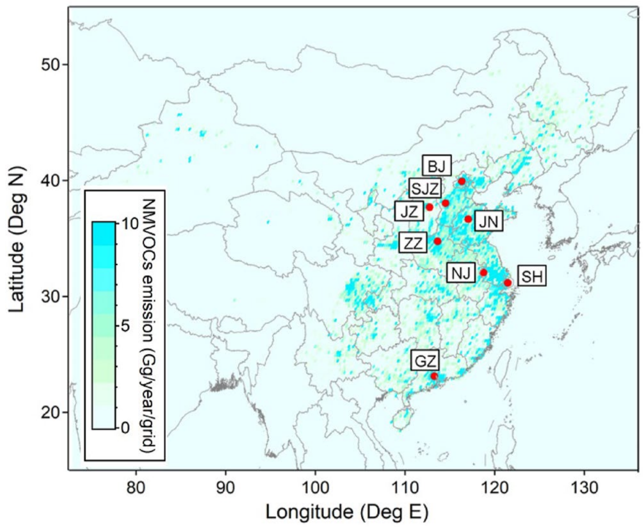

Figure 1. Map showing the locations of major Chinese cities analyzed in this study. The names for individual cities are as follows. BJ: Beijing; SJZ: Shijiazhuang; JN: Ji'nan; ZZ: Zhengzhou; JZ: Jinzhong; NJ: Nanjing; SH: Shanghai; GZ: Guangzhou. The emission data of NMVOCs (non-methane volatile organic compounds) were taken from Li et al. (2017).

There is a large variety of VOCs species in the ambient air, and their contributions to O_3 formation vary largely depending on both chemical reactivity and mass/concentration (Guo et al., 2017). Integrated scales taking both chemical reactivity and mass/concentration into consideration are in high demand to provide scientific support for VOCs management and O_3 pollution control. One of the widely used metrics is the ozone formation potential (OFP), and its definition and calculation varied among literature (Chang & Rudy, 1990; Jenkin et al., 2017; NRC, 1999; Russell et al., 1995). Currently, the OFP is usually defined as the product of incremental reactivity (IR) multiplying by emission quantity (i.e., emission-weighted OFP) (Li et al., 2019; Sha et al., 2021; Shi et al., 2022) or observation data (i.e., concentration-weighted OFP (Conw_OFP)) (Mo et al., 2022; Pei et al., 2022; Shi et al., 2022). The IR values are generally determined by model simulations (Carter, 1994a, 1994b, 2009, 2010; Qiu et al., 2020; Venecek et al., 2018; Zhang et al., 2021) and then can be used for the OFP calculation. The choice of IR scale is heavily dependent on the NO_x condition (Carter, 1994b; Zhang et al., 2021), for example, the maximum incremental reactivity (MIR), maximum O_3 reactivity (MOR), and equal benefit incremental reactivity (EBIR) scales are most appropriate for application in VOCs-limited (high-NO_x conditions), mixed-limited (median-NO_x), and NO_x-limited (low-NO_x) areas, respectively. A rough application of MIR scales to identify reactive VOCs species or calculate OFPs in NO_x-limited regimes (generally rural or remote areas) would result in large uncertainties (Zhang et al., 2021).

Most of the Chinese urban areas are currently under high-NO_x environment (Lu et al., 2019; Wang et al., 2022), and thereby, the MIR scales are appropriate for application. The existing studies in China tended to directly adopt the MIR scales developed by Carter (2010) for the U.S. urban conditions (Li et al., 2019; Mo et al., 2020; Shi et al., 2022), owing to the lack of localized results. Such simplified adoption has introduced some concerns, since there is a large discrepancy in the atmospheric conditions between China and the U.S. (Li et al., 2019; Venecek et al., 2018). Recently, some studies developed the localized MIR scales in Chinese cities and found a nonnegligible discrepancy between the localized results and those built upon the U.S. scenarios (Qiu et al., 2020; Zhang et al., 2021, 2022). Further inspection revealed that the differences in chemical mechanisms (RACM vs. MCM vs. SAPRC) and/or environmental conditions between China and U.S. were possible reasons for the discrepancy. However, the above comparison is not sufficient to reflect the real difference between China and the U.S., due to the very limited number of urban scenarios in China. Analogously, more Chinese urban scenarios are needed to see how VOCs reactivity differ among major cities of China, and to confirm whether the MIRs constructed based on regional average scenarios could serve as a general scale that can apply to a large variety of urban areas. Addressing this point has great significance to VOCs management and O_3 pollution control, especially over areas suffering from the lack of localized IR products.

In this study, we adopted the Master Chemical Mechanism version 3.3.1 (MCMv3.3.1) box model to establish the localized MIR scales in 8 major cities over Central-Eastern China (Figure 1). We first present the typical environmental conditions during the O_3 pollution episodes (defined as the day with the maximum daily 8-hr average O_3 (MDA8 O_3) mixing ratio exceeding the Class II Chinese National Ambient Air Quality Standard (i.e., 160 $\mu g \cdot m^{-3}$)). We then examine the representativeness of regional average MIR scales and compare them with those constructed based on the U.S. urban conditions. Finally, we quantify the Conw_OFP for VOCs based on the Chinese localized MIRs and identify key species together with their sources to provide scientific and effective support for VOCs management across China.

2. Materials and Methods

2.1. Study Areas and Observation Data

The information of study areas and observation data used for the MIR calculation are summarized in Figure 1 and Table 1. Totally 8 sets of observations were involved. These observations were conducted in urban areas of major Chinese cities, and the observation periods were concentrated around July–September 2020 (apart from

Table 1
Overview of Urban Field Observations Used for MIR Calculation in the Present Study

Region	Site	Location	Observation period	MDA8 O_3 non-attainment frequency
Beijing-Tianjin-Hebei and surrounding areas	Beijing	116.33°E, 39.94°N	1 August to 20 September 2020	29%
	Shijiazhuang	114.53°E, 38.06°N	1 July to 20 September 2020	50%
	Ji'nan	117.05°E, 36.66°N	1 July to 13 September 2020	43%
	Zhengzhou	113.61°E, 34.75°N	1 July to 20 September 2020	29%
Fenwei Plain	Jinzhong	112.73°E, 37.71°N	1 July to 20 September 2020	29%
Yangtze River Delta	Nanjing	118.75°E, 32.06°N	1 July to 20 September 2020	21%
	Shanghai	121.45°E, 31.17°N	10 August to 20 September 2020	17%
Pearl River Delta	Guangzhou	113.27°E, 23.12°N	1 January 2018 to 31 December 2019	-

Note. The information of observations in Guangzhou were taken from Zhang et al. (2021). Here MDA8 O_3 non-attainment day is defined as a day with MDA8 O_3 concentration exceeding 160 $\mu g \cdot m^{-3}$.

Guangzhou). The selected cities are both economically developed and densely populated, and located in representative regions suffering from serious O_3 pollution, such as Beijing, Shijiazhuang, Ji'nan, and Zhengzhou in Beijing-Tianjin-Hebei and surrounding areas (BTHs), Jinzhong in Fenwei Plain (FWP), and Nanjing and Shanghai in the Yangtze River Delta (YRD). The MIRs in Guangzhou (located in the Pearl River Delta (PRD)) were calculated previously (Zhang et al., 2021) and directly used for analyses in this study. Scenarios for the 8 major cities should have a good representation of a large variety of urban environments over Central-Eastern China (Figure 1).

Real-time measurement data of trace gases, VOCs, and meteorological parameters were obtained to drive the MIR calculation. Briefly, the data of trace gases, including O_3, NO_2, SO_2, and CO, were obtained from the national air-quality monitoring stations (https://air.cnemc.cn:18007/). These species were routinely monitored by commercial instruments with strict quality assurance and quality control procedures (CNEMC, 2018). The data of VOCs were obtained from the local Environmental Protection Agencies, where 57 compounds (including 29 alkanes, 10 alkenes, 1 alkyne, and 17 aromatics) prescribed by the Photochemical Assessment Monitoring Stations (PAMS) of U.S. Environmental Protection Agency were detected in real-time by commercial GC-FID/MS VOC analyzers with strict quality assurance and control procedures (CNEMC, 2019). Meteorological parameters including temperature, relative humidity, and pressure were obtained from the China Meteorological Data Service Center (http://data.cma.cn).

2.2. Calculation of MIRs for VOCs

A chemical box model constructed on the F0AM (Framework for 0-D Atmospheric Modeling) platform was applied for the MIR calculation (Wolfe et al., 2016). The model was based on the MCMv3.3.1, a gas-phase chemical mechanism that near-explicitly describes the degradation reactions of 143 primary VOCs (Jenkin et al., 2003, 2015; Saunders et al., 2003). Physical processes including solar radiation, planetary boundary layer evolution, dry deposition, and exchange with background air were also considered within the model. Detailed information of model configuration has been provided in previous studies (Xue et al., 2013; Zhang et al., 2021).

As Table 2 shows, 8 scenarios (including 7 Base Case Scenarios for individual cities and 1 Averaged Chinese Urban Condition Scenario) were designed for the MIR calculation. For Base Case Scenarios, the median diurnal profiles of NO_2, CO, SO_2, HONO, C_1–C_{12} VOCs, oxygenated VOCs (OVOCs), temperature, relative humidity, and pressure on O_3 episode days of each city were processed as 1-day model inputs to constrain the model. Observation data for most of the above species and parameters were available, and those without available data but with large importance (e.g., HONO and OVOCs, as demonstrated by Chen et al. (2020), Gu et al. (2022), and Gu et al. (2020)) were processed as follows. The HONO input was assumed to be 2% of NO_2 concentrations, and the 1-day OVOCs input and initial concentrations of OH and HO_2 radicals were approximated as model-simulated values with pre-run of 2 days. The inputs of Averaged Chinese Urban Condition Scenario were obtained by averaging 1-day model inputs for the 7 Base Case Scenarios and Base Case Scenario for Guangzhou. The model was initiated at 6:00 local time (LT), and the integration had a step of 1 hr and duration of 1 day. For consistency

Table 2
Summary of Atmospheric Conditions for the Averaged Chinese Urban Condition Scenario (AveCon) and Base Case Scenarios for Individual Cities

Site	NO_x (ppbv)	VOCs (ppbv)	Temperature (°C)	Relative humidity (%)	VOCs/NO_x (ppbv/ppbv)	$[NO_x]_{MIR}$/$[NO_x]_{BASE}$	$[NO_x]_{MOR}$/$[NO_x]_{BASE}$	$[NO_x]_{EBIR}$/$[NO_x]_{BASE}$
Beijing	9.3 ± 4.3	18.2 ± 2.7	27.8 ± 3.1	66 ± 12	2.2 ± 0.6	1.15	0.59	0.27
Shijiazhuang	14.0 ± 4.9	33.4 ± 3.6	27.2 ± 3.3	70 ± 12	2.6 ± 0.7	1.86	0.94	0.36
Ji'nan	13.8 ± 4.9	20.0 ± 3.9	26.2 ± 3.7	67 ± 14	1.5 ± 0.3	1.10	0.56	0.26
Zhengzhou	18.7 ± 6.4	29.2 ± 4.7	27.0 ± 3.3	73 ± 19	1.7 ± 0.4	1.34	0.66	0.26
Jinzhong	13.9 ± 4.9	14.6 ± 2.1	24.0 ± 4.3	60 ± 16	1.2 ± 0.4	0.79	0.40	0.22
Nanjing	13.3 ± 5.3	20.3 ± 3.6	28.2 ± 3.8	70 ± 21	1.8 ± 0.7	1.75	0.75	0.32
Shanghai	23.4 ± 5.3	30.2 ± 5.9	28.5 ± 3.1	58 ± 14	1.4 ± 0.4	1.04	0.54	0.27
Guangzhou	30.7 ± 8.9	26.7 ± 4.9	27.7 ± 3.7	48 ± 14	1.0 ± 0.5	1.15	0.60	0.28
AveCon	15.8 ± 4.6	25.5 ± 3.3	27.0 ± 3.3	65 ± 15	1.7 ± 0.4	1.37	0.69	0.30

Note. The NO_x conditions for Base Case, MIR, MOR, and EBIR scenarios were presented as $[NO_x]_{BASE}$, $[NO_x]_{MIR}$, $[NO_x]_{MOR}$, and $[NO_x]_{EBIR}$, respectively. The NO_2 concentrations were used as a proxy for NO_x concentrations for all cities apart from Guangzhou.

with Carter (1994a, 1994b), we extracted simulation results during 6:00–16:00 LT for the MIR calculation. The O_3 concentrations were initialized using median value observed at 6:00 LT on O_3 episode days, and then O_3 chemistry and concentrations were simulated freely with inputs of related species and parameters in the following integration.

There were two major procedures for IR calculation (Carter, 1994a, 1994b, Zhang et al., 2021), that is, NO_x-adjusted runs and VOCs-adjusted runs. The NO_x-adjusted runs were performed to determine the exact NO_x inputs for MIR, MOR, and EBIR scenario as well as to diagnose the O_3 formation regimes (an example was provided in Figure S1 in Supporting Information S2). For a given city, $[NO_x]_{MOR}$ (i.e., the NO_x conditions under MOR scenario) represents the boundary between the VOCs-limited and mixed-limited O_3 formation regime, and $[NO_x]_{EBIR}$ (i.e., the NO_x conditions under EBIR scenario) represents the boundary between the mixed-limited and NO_x-limited O_3 formation regime. Then, the O_3-NO_x-VOC sensitivity can be determined by comparison between $[NO_x]_{BASE}$ (i.e., the NO_x conditions under Base Case Scenario) against $[NO_x]_{MOR}$ and $[NO_x]_{EBIR}$. As documented in Table 2, the comparison between $[NO_x]_{BASE}$ against $[NO_x]_{MOR}$ and $[NO_x]_{EBIR}$ indicates that the O_3 formation persists in VOCs-limited and NO_x-saturated regime in major Chinese cities, and thus the MIRs are suitable for application. Note that $[NO_x]_{BASE}$ for Shijiazhuang is very close to $[NO_x]_{MOR}$, which indicates that the applied IRs should be updated over a short period along with changes in the chemical regimes of O_3 formation.

In the second procedure, we calculated the localized MIRs for individual VOC species by VOCs-adjusted runs (including VOCs-base runs and VOCs-addition runs). We adopted the same method as introduced by Zhang et al. (2021) to determine and quantify the addition mass of the target VOC ($\triangle VOC_i$ in Equation 1). With prescribed NO_x inputs for a MIR scenario, a series of VOCs-base runs and VOCs-addition runs were performed. For a given species, the model-simulated maximum concentrations of O_3 in VOCs-base runs and VOCs-addition runs were extracted for the MIR calculation ($\triangle O_3$ in Equation 1). The MIR values for totally 46 PAMS species were directly determined according to Equation 1. Due to the unavailable degradation chemistry in the MCM v3.3.1, the MIRs for the other 11 PAMS species were indirectly estimated by using their associated k_{OH} (see Table S1 in Supporting Information S3) and approximating their degradation chemistry to the mechanism of the identified surrogate VOCs. The identified surrogate VOCs were *i*-pentane (for cyclopentane), cyclohexane (for methyl cyclopentane), 2-methyl hexane (for 2,4-dimethyl pentane and 2,3-dimethyl pentane), *n*-heptane (for methyl cyclohexane), *n*-octane (for 2,2,4-trimethyl pentane, 2,3,4-trimethyl pentane, 2-methyl heptane, and 3-methyl heptane), *m*-ethyl toluene (for *m*-diethyl benzene), and *p*-ethyl toluene (for *p*-diethyl benzene), in consideration of both carbon numbers and functional groups.

$$MIR_i = \frac{\triangle O_3}{\triangle VOC_i} \quad (1)$$

where MIR_i represents the MIR value of VOC_i, $\triangle O_3$ is the mass of additional O_3 formed (unit: μg·m^{-3}), and $\triangle VOC_i$ is the mass of VOC_i added to the scenario (unit: μg·m^{-3}).

In the present modeling, the NO concentrations were not treated as model constraints due to lack of available NO data (except for Guangzhou), instead, the NO evolution and chemistry were determined with constraints of related species or parameters during each integration step. As shown in Figure S2 in Supporting Information S2, the model-simulated NO concentrations were overall comparable to the measured data during the daytime in Guangzhou. Sensitivity test was conducted by taking Guangzhou as a case to evaluate the uncertainty caused by such treatment on the MIR scales. As shown in Figure S1 in Supporting Information S2, the MIRs obtained from sensitivity test showed strong correlations with those obtained from base scenario (R^2: 0.96), but the lack of NO data would result in lower MIR values (by −10%), which should be attributed to the higher VOCs/NO_x ratios in sensitivity test (see Section 3.2).

2.3. Calculation of OFPs for VOCs

The localized MIR values were applied to quantify the Conw_OFPs for VOCs according to Equation 2 (Mo et al., 2022; Pei et al., 2022).

$$\text{Conw\_OFP}_i = [\text{VOC}_i] * \text{MIR}_i \quad (2)$$

where Conw_OFP_i represents the Conw_OFP value of VOC_i, MIR_i is the above-calculated MIR value of VOC_i, and [VOC_i] represents the observed concentrations of VOC_i. Caution should be taken when using observation data to quantify the OFPs, since such treatment would somewhat underestimate the importance of reactive VOCs to O_3 production (Zhang et al., 2021, 2022). To better reflect local emission characteristics, we used averages of observation data for anthropogenic VOCs during 6:00–7:00 LT and for biogenic VOCs during 12:00–14:00 LT for the Conw_OFP calculation.

3. Results and Discussion

3.1. Overview of Urban Ozone Pollution Scenarios

During the observation period, the O_3 pollution showed a clear spatial distribution pattern (Table 1). In the YRD region, a MDA8 O_3 non-attainment frequency (defined as days with MDA8 O_3 > 160 μg·m^{-3}) of 17% was recorded in Shanghai during the 42-day campaign, and of 21% was recorded in Nanjing during the 82-day campaign. The O_3 pollution situation in Shanghai seemed to be lighter than Nanjing and the other cities, partly owing to its strong NO titration effect (see Figure S3 in Supporting Information S2 for the time series of NO_2 and O_3 concentrations) (Xue et al., 2014). In the FWP region, a MDA8 O_3 non-attainment frequency of 29% was recorded in Jinzhong during the 82-day campaign. The urban O_3 pollution situation in the BTHs region was more serious than that in the above two regions. For example, a MDA8 O_3 non-attainment frequency of 29% and 50% was recorded in Zhengzhou and Shijiazhuang, respectively, during the 82-day campaign, of 30% was recorded in Beijing during the 50-day campaign, and of 43% was recorded in Ji'nan during the 75-day campaign. A comparison with the monitoring results in developed countries indicates the serious O_3 pollution situation in China. On one hand, the number of days with MDA8 O_3 > 150 μg·m^{-3} (a benchmark level for the U.S.) recorded in these Chinese cities during the campaigns (short than 3 months) was even larger than that in most U.S. and European urban sites determined on an annual basis (Figure S4 in Supporting Information S2) (Fleming et al., 2018). On the other hand, the average diurnal O_3 amplitudes (54–67 ppbv; defined as the daily maximum minus the minimum O_3 concentration recorded prior to the daily maximum) (Xu et al., 2020) were even larger than those recorded in Los Angeles (<50 ppbv in August 2016) (Solomon et al., 2020), a megacity widely recognized to suffer from serious O_3 pollution. In particular, the average diurnal O_3 amplitudes were even enhanced to 76–96 ppbv over Chinese urban areas on episode days, indicating a strong in situ O_3 formation capacity.

The observed chemical environments and meteorological parameters were presented and compared (Table 2). The PRD region was included for comparison and the data of Guangzhou were obtained from Zhang et al. (2021). For all city-clusters, the meteorological parameters showed similar characteristics with warm temperatures (24.0–28.5°C) and moderate relative humidity (58%–73%). Such weather conditions are conducive to O_3 formation and typical of O_3 episodes (Liu & Wang, 2020a). The diurnal patterns of NO_x and VOCs were similar among

10.1029/2022JD037296

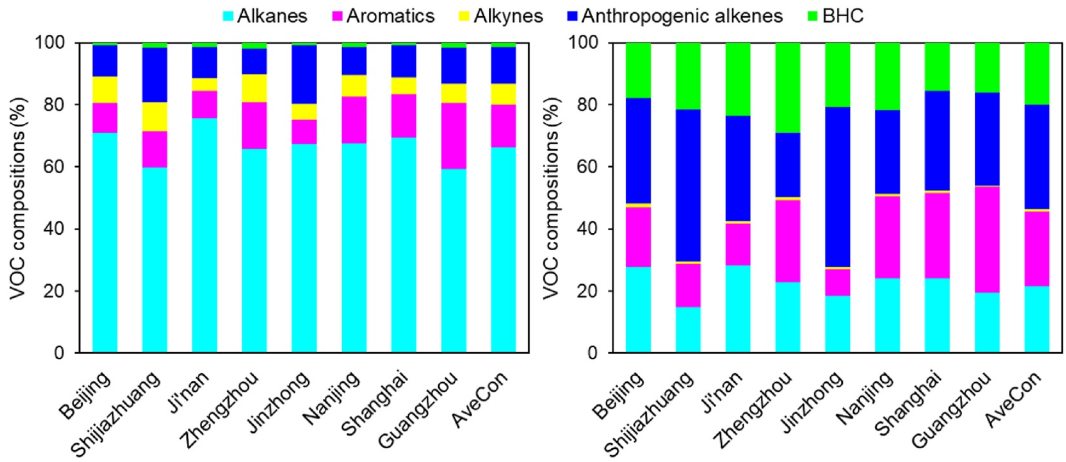

Figure 2. VOCs compositions of concentrations (ppbv/ppbv; the left panel) and OH reactivities (s^{-1}/s^{-1}; the right panel) in the Averaged Chinese Urban Condition Scenario (AveCon) and the Base Case Scenarios for individual cities. The VOCs data of Guangzhou were taken from Zhang et al. (2021). The k_{OH} data were obtained from Jenkin et al. (2018a, 2018b), McGillen et al. (2020), Atkinson and Arey (2003) and EPA Atmospheric Oxidation Program estimation (see details in Table S1 in Supporting Information S3).

individual cities with bimodal morning and evening concentration peaks (Figure S5 in Supporting Information S2), owing to a combined influence of shallow boundary layer and intense traffic emissions at rush hours. However, the magnitudes of NO_x and VOCs differed largely between cities, even within the same city-cluster. For example, the average NO_2 and VOCs concentrations (±standard deviation) were 23.4 ± 5.3 ppbv and 30.2 ± 5.9 ppbv in Shanghai, respectively, higher than those observed in Nanjing (NO_2: 13.3 ± 5.3 ppbv; VOCs: 20.3 ± 3.6 ppbv). Besides, the spatial distributions of NO_x and VOCs were not that consistent. The highest average NO_2 concentrations were observed in Guangzhou (27.1 ± 3.6 ppbv) and Shanghai (23.4 ± 5.3 ppbv), with the lowest observed in Beijing (9.3 ± 4.3 ppbv). In comparison, the highest average VOCs concentrations were observed in Shijiazhuang (33.4 ± 3.6 ppbv) and Shanghai (30.2 ± 5.9 ppbv), with the lowest observed in Jinzhong (14.6 ± 2.1 ppbv). This inconsistency led to a wide distribution of average VOCs/NO_x ratios (ppbv/ppbv), which ranged from 1.0 ± 0.5 in Guangzhou to 2.6 ± 0.7 in Shijiazhuang. As described in Section 2.2, we also examined the relative availability of NO_x and VOCs with application of the MCM chemical box model (i.e., by the NO_x-adjusted runs) and found a widespread existence of VOCs-limited O_3 formation regime in selected Chinese cities. The results demonstrate the importance of VOCs to O_3 formation in urban areas of Central-Eastern China, and thereby highlight the need for localizing MIRs to quantitatively evaluate the contributions of different VOCs species to O_3 formation.

The detailed VOCs chemical compositions (classified into alkanes, anthropogenic alkenes, aromatics, alkynes, and biogenic VOCs (BHC)) were examined (Figure 2). Overall, alkanes were the dominant class based on observed concentrations (59%–76%). A very interesting result is the increasing contributions of aromatics to total VOCs along with a lower latitude (though not strictly), reflecting the distinct industrial structures and VOCs emission sources over individual areas. For instance, the average fraction of aromatics was 10 ± 2% in Beijing, which increased to 15 ± 4% and 21 ± 2% in Nanjing and Guangzhou, respectively. Anthropogenic alkenes were the dominant class based on OH reactivities (L_{OH}), which is the product of VOCs concentration and its reaction rate constant with OH radical. Specifically, anthropogenic alkenes were the dominant reactive class in Beijing (35 ± 2%), Shijiazhuang (51 ± 7%), Ji'nan (34 ± 8%), Jinzhong (51 ± 16%), Nanjing (27 ± 8%), and Shanghai (33 ± 3%), while aromatics played a dominant role in Guangzhou (34 ± 6%) and BHC dominated in Zhengzhou (26 ± 24%). The results underline the large variance in chemical environments among Chinese cities, the effects of which on MIRs will be discussed in Section 3.2.

3.2. Localized MIRs for VOCs in China

Figure 3 and Table 3 present the localized MIRs for 57 PAMS species. The distribution of MIRs among VOCs species was generally the same for the involved city scenarios. Within the defined major VOCs groups, the MIR

10.1029/2022JD037296

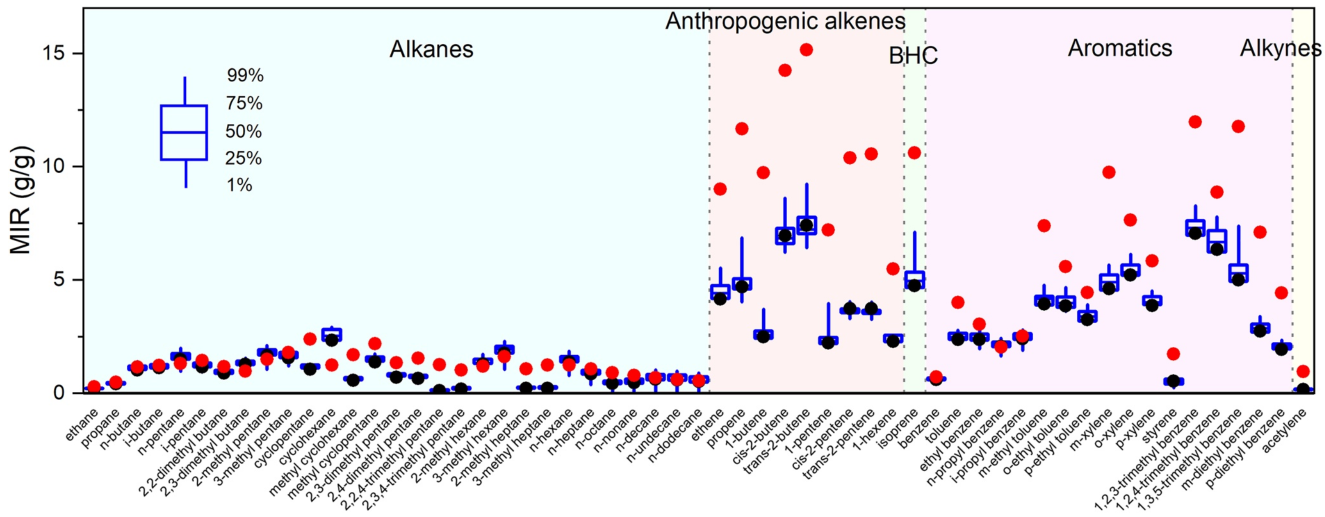

Figure 3. Distribution of MIRs for 57 individual PAMS species over eight major Chinese cities (indicated by the blue box and whiskers) and comparison with those obtained from the Averaged Chinese Urban Condition Scenario (the black circles) and with the extensively used U.S. MIRs (the red circles). The box plot provides the 1%, 25%, 50%, 75%, and 99% the data. The MIRs for VOCs in Guangzhou and U.S. were obtained from Zhang et al. (2021) and Carter (2010), respectively.

values for anthropogenic alkenes (2.18–9.27 g/g), BHC (4.62–7.09 g/g), and aromatics (0.24–8.27 g/g) were large, while those for alkanes (−0.04–2.91 g/g) and alkynes (0.15–0.22 g/g) were relatively small. The MIRs for species within aromatic class showed wider distributions than alkene class, mainly due to the low reactivity of benzene (0.49–0.73 g/g) and styrene (0.24–0.70 g/g). On species level, *trans*-2-butene (6.42–9.27 g/g), *cis*-2-butene (6.21–8.58 g/g), 1,2,3-trimenthyl benzene (6.90–8.27 g/g), 1,2,4-trimenthyl benzene (6.16–7.81 g/g), 1,3,5-trimenthyl benzene (4.87–7.47 g/g), isoprene (4.62–7.09 g/g), propene (4.03–6.83 g/g), *o*-xylene (5.06–6.13 g/g), *m*-xylene (4.50–5.72 g/g), and ethene (4.07–5.54 g/g) ranked as the top 10 reactive species, but the exact ranks differed slightly among individual cities.

The localized MIRs constructed based on individual cities and the Averaged Chinese Urban Condition were compared to evaluate the representativeness of regional average MIRs (Figure 3 and Figure S6 in Supporting Information S2). A strong correlation in MIRs for 57 PAMS species was shown by the linear regression analysis with R^2 in the range of 0.94–1.00, which was also the case specific to individual major VOCs groups (R^2 for alkanes: 0.83–1.00; anthropogenic alkenes: 0.95–1.00; and aromatics: 0.92–1.00). Despite a strong correlation, the magnitudes of MIRs showed discrepancy. Taking the MIRs obtained from the Averaged Chinese Urban Condition as a benchmark (i.e., *x*-axis), the MIRs for VOCs in Ji'nan showed the lowest RMA (reduced major axis) (Leduc, 1987) slope (0.95), while those in Guangzhou showed the largest RMA slope (1.35), and the RMA slopes exhibited by the other cities fell in the range of 0.97–1.11. The obviously higher MIR values in Guangzhou should be attributed to its lower VOCs/NO_x ratio (1.0) and higher aromatics contribution (21%) (other cities: 1.2–2.6 for VOCs/NO_x ratio and 8%–15% for aromatics contribution) (see Table 2 and Figure 2). Under high NO_x conditions, a lower VOCs/NO_x ratio tends to enhance the importance of VOCs to O_3 formation, and a larger contribution of aromatics (together with their chemical degradation products) tends to strengthen NO_x sinks and hence promotes O_3 formation (i.e., higher MIR values) (Zhang et al., 2021). It should be noted that the different treatment of input for NO_x and OVOCs between this study and Zhang et al. (2021) might exert effects on the VOCs/NO_x ratio. We used the NO_2 concentrations as a proxy for NO_x input and approximated the OVOCs input as model-simulated values, while Zhang et al. (2021) used real NO_x concentrations as input and approximated the input for major OVOC species as 0.10 ppbv, which somewhat contributed to the lower VOCs/NO_x ratio in Guangzhou scenarios. On species level, the MIRs of *n*-octane, *n*-nonane, *n*-decane, *n*-undecane, and *n*-dodecane showed the largest variability (see coefficient of variation in Table 3), due to their strong dependence on the chemical environmental conditions (Zhang et al., 2021).

Overall, the MIRs obtained from the Averaged Chinese Urban Condition are well representative of those obtained from the individual cities apart from Guangzhou, which indicates that the regional representative MIR scales

Table 3
Tabulation of MIRs (g O_3/g VOC) for VOCs in Individual Cities and Averaged Chinese Urban Condition Scenario (Represented as AveCon)

Species	BJ	SJZ	JN	ZZ	JZ	NJ	SH	GZ	Ave ± VD	AveCon
Ethane	0.23	0.27	0.23	0.19	0.21	0.20	0.22	0.19	0.22 ± 0.12	0.19
Propane	0.48	0.55	0.47	0.41	0.43	0.42	0.46	0.25	0.43 ± 0.20	0.42
n-Butane	1.22	1.40	1.17	1.00	1.08	1.08	1.17	0.83	1.12 ± 0.15	1.03
i-Butane	1.30	1.41	1.23	1.09	1.19	1.14	1.22	0.91	1.19 ± 0.12	1.12
n-Pentane	1.80	1.99	1.71	1.44	1.57	1.58	1.71	0.94	1.59 ± 0.20	1.49
i-Pentane	1.36	1.51	1.30	1.14	1.23	1.20	1.28	0.93	1.24 ± 0.14	1.16
Cyclopentane	1.25	1.17	1.25	0.99	1.19	1.11	1.19	–	1.16 ± 0.08	1.05
n-Hexane	1.64	1.85	1.60	1.34	1.42	1.46	1.58	0.75	1.46 ± 0.22	1.37
2,2-Dimethyl butane	1.04	1.15	0.99	0.86	0.91	0.93	1.00	0.67	0.94 ± 0.15	0.88
2,3-Dimethyl butane	1.46	1.56	1.39	1.24	1.31	1.31	1.35	0.75	1.30 ± 0.19	1.27
2-Methyl pentane	1.99	2.11	1.87	1.63	1.77	1.75	1.84	1.04	1.75 ± 0.18	1.67
3-Methyl pentane	1.85	2.02	1.77	1.52	1.65	1.63	1.75	1.18	1.67 ± 0.15	1.56
Cyclohexane	2.91	2.81	2.52	2.31	2.34	2.80	2.53	–	2.60 ± 0.09	2.33
Methyl cyclopentane	1.74	1.48	1.58	1.29	1.42	1.60	1.53	–	1.52 ± 0.09	1.37
n-Heptane	1.00	1.22	1.03	0.85	0.83	0.90	0.98	0.34	0.89 ± 0.29	0.85
2,3-Dimethyl pentane	0.85	0.80	0.91	0.65	0.80	0.76	0.86	–	0.80 ± 0.10	0.71
2,4-Dimethyl pentane	0.78	0.73	0.84	0.60	0.74	0.69	0.80	–	0.74 ± 0.11	0.65
2-Methyl hexane	1.51	1.73	1.50	1.26	1.32	1.36	1.48	–	1.45 ± 0.11	1.29
3-Methyl hexane	2.11	2.30	2.03	1.71	1.84	1.88	2.01	1.04	1.87 ± 0.20	1.76
Methyl cyclohexane	0.69	0.62	0.80	0.49	0.65	0.60	0.70	–	0.65 ± 0.15	0.56
n-Octane	0.52	0.69	0.58	0.48	0.38	0.50	0.49	−0.00	0.46 ± 0.45	0.44
2,2,4-Trimethyl pentane	0.14	0.13	0.20	0.10	0.13	0.11	0.16	–	0.14 ± 0.25	0.11
2,3,4-Trimethyl pentane	0.24	0.20	0.32	0.15	0.21	0.19	0.25	–	0.23 ± 0.25	0.18
2-Methyl heptane	0.28	0.23	0.37	0.17	0.25	0.23	0.28	–	0.26 ± 0.24	0.21
3-Methyl heptane	0.28	0.23	0.38	0.17	0.25	0.23	0.29	–	0.26 ± 0.24	0.21
n-Nonane	0.57	0.78	0.65	0.50	0.40	0.57	0.59	−0.02	0.51 ± 0.44	0.47
n-Decane	0.80	1.03	0.86	0.63	0.57	0.75	0.81	0.06	0.69 ± 0.42	0.62
n-Undecane	0.78	0.98	0.83	0.60	0.54	0.75	0.78	−0.00	0.66 ± 0.45	0.59
n-Dodecane	0.71	0.90	0.76	0.53	0.47	0.69	0.70	−0.04	0.60 ± 0.44	0.52
Ethene	4.78	4.72	4.33	4.07	4.50	4.18	4.17	5.54	4.54 ± 0.11	4.16
Propene	5.24	4.88	4.60	4.64	4.85	4.03	4.60	6.83	4.96 ± 0.17	4.69
1-Butene	2.81	2.70	2.40	2.46	2.53	2.59	2.35	3.77	2.70 ± 0.17	2.48
cis-2-Butene	6.98	6.87	6.59	6.62	6.21	6.81	7.58	8.58	7.03 ± 0.11	6.95
trans-2-Butene	7.40	7.23	7.04	7.05	6.42	7.22	8.13	9.27	7.47 ± 0.12	7.41
1-Pentene	2.50	2.44	2.18	2.19	2.26	2.32	2.18	3.93	2.50 ± 0.24	2.22
cis-2-Pentene	3.72	3.68	3.56	3.55	3.28	3.67	4.05	–	3.64 ± 0.06	3.74
trans-2-Pentene	3.65	3.64	3.55	3.52	3.26	3.66	4.03	–	3.62 ± 0.06	3.73
Isoprene	5.38	5.30	4.67	4.66	4.97	4.94	4.62	7.09	5.20 ± 0.16	4.75
1-Hexene	2.56	2.56	2.29	2.24	2.30	2.44	2.27	–	2.38 ± 0.06	2.28
Benzene	0.68	0.73	0.65	0.59	0.62	0.59	0.68	0.49	0.63 ± 0.12	0.61
Toluene	2.79	2.72	2.49	2.32	2.57	2.42	2.47	2.33	2.51 ± 0.07	2.37
Ethyl benzene	2.81	2.63	2.45	2.32	2.60	2.42	2.38	1.95	2.45 ± 0.10	2.37

Table 3
Continued

Species	BJ	SJZ	JN	ZZ	JZ	NJ	SH	GZ	Ave ± VD	AveCon
m-Xylene	5.46	4.96	4.59	4.52	4.99	4.86	4.50	5.72	4.95 ± 0.09	4.61
o-Xylene	6.13	5.62	5.30	5.06	5.72	5.40	5.23	5.20	5.46 ± 0.06	5.21
p-Xylene	4.52	4.26	3.98	3.74	4.19	4.02	3.91	–	4.09 ± 0.06	3.87
Styrene	0.53	0.70	0.52	0.60	0.24	0.66	0.47	0.46	0.52 ± 0.27	0.53
n-Propyl benzene	2.43	2.30	2.17	2.00	2.23	2.12	2.16	1.61	2.13 ± 0.11	2.07
i-Propyl benzene	2.80	2.68	2.51	2.32	2.59	2.45	2.52	1.87	2.47 ± 0.11	2.40
m-Ethyl toluene	4.77	4.19	3.90	3.89	4.36	4.14	3.74	4.23	4.15 ± 0.08	3.94
o-Ethyl toluene	4.67	4.18	3.92	3.77	4.30	4.03	3.81	3.61	4.04 ± 0.08	3.86
p-Ethyl toluene	3.91	3.54	3.34	3.17	3.60	3.39	3.19	–	3.45 ± 0.08	3.24
1,2,3-Trimethyl benzene	8.27	7.53	7.02	6.90	7.70	7.34	6.94	7.25	7.37 ± 0.06	7.06
1,2,4-Trimethyl benzene	7.43	6.74	6.26	6.22	6.94	6.59	6.16	7.81	6.77 ± 0.09	6.35
1,3,5-Trimethyl benzene	5.93	5.41	4.87	4.98	5.26	5.34	4.90	7.47	5.52 ± 0.16	5.00
m-Diethyl benzene	3.39	2.99	2.82	2.70	3.06	2.86	2.69	–	2.93 ± 0.08	2.74
p-Diethyl benzene	2.34	2.12	2.07	1.86	2.17	1.99	1.96	–	2.07 ± 0.08	1.93
Acetylene	0.19	0.20	0.17	0.15	0.18	0.15	0.17	0.22	0.18 ± 0.04	0.16

Note. Also shown are the averages and coefficient of variation for MIRs in individual cities (represented as Ave ± VD). The MIR values for VOCs in Guangzhou were obtained from Zhang et al. (2021).

could serve as approximate reactivities in urban areas of Central-Eastern China, as long as their chemical environments and meteorology of O_3 episodes days are not largely different.

3.3. Comparison With the MIR Scales in the U.S.

The MIRs constructed based on Averaged Chinese and U.S. Urban Conditions were compared (Figure 3) to infer the difference in VOC reactivities between China and the U.S. The U.S. MIRs were obtained from Carter (2010), which were calculated based upon the 1988 U.S. pollution scenario and have been extensively used in previous studies. A strong correlation was shown in MIRs for the 57 PAMS species (R^2: 0.83) between China and the U.S., despite difference in environmental conditions and chemical mechanisms (MCM v3.3.1 vs. SAPRC07). However, the localized MIRs in China were significantly lower than U.S. MIRs (by 119%, $p < 0.01$, tested by the one-way analysis of variance method). Such large discrepancy in MIR magnitudes should partly be attributed to the interference introduced by model inputs, since MIRs obtained from observation-based inputs (adopted in this study) tended to be lower than those from emission-based inputs (adopted in Carter (2010)), as demonstrated in Zhang et al. (2021).

The relative reactivity (RR) scale is defined as the IR value for a given species divided by that for a reference species (Carter, 1994b). It can minimize the interference introduced by background conditions and hence was chosen for further comparison to infer the difference in VOCs reactivity between China (referred to as CHN_MCM; constructed based on the Averaged Chinese Urban Conditions) and the U.S (Figure 4). Ethene was selected as a reference species for consistency with Derwent et al. (2010). The U.S. RRs were actually constructed based on California scenarios, whose satisfactory ability to represent the Averaged U.S. Urban Condition has been demonstrated in Zhang et al. (2021). Two sets of U.S. RR values were chosen for comparison, with one developed using SAPRC07 (US_SAPRC) (Carter, 2010) and the other developed using MCM v3.1 (US_MCM) (Derwent et al., 2010), but the MIRs for the selected 44 species (whose MIR values were calculated for both Chinese and U.S. Urban Conditions) derived from them were fairly similar (RMA slope: 0.92; R^2: 0.94). Analogously, a strong correlation was found in RRs for these 44 species between CHN_MCM and US_SAPRC/MCM, as indicated by R^2 (US_MCM: 0.84; US_SAPRC: 0.79). The correlation was improved with the same chemical mechanism (i.e., MCM), elucidating the influence of different representations for VOCs degradation between MCM and SAPRC. We further examined the comparison results for major VOCs groups (i.e., alkanes (18 species), alkenes

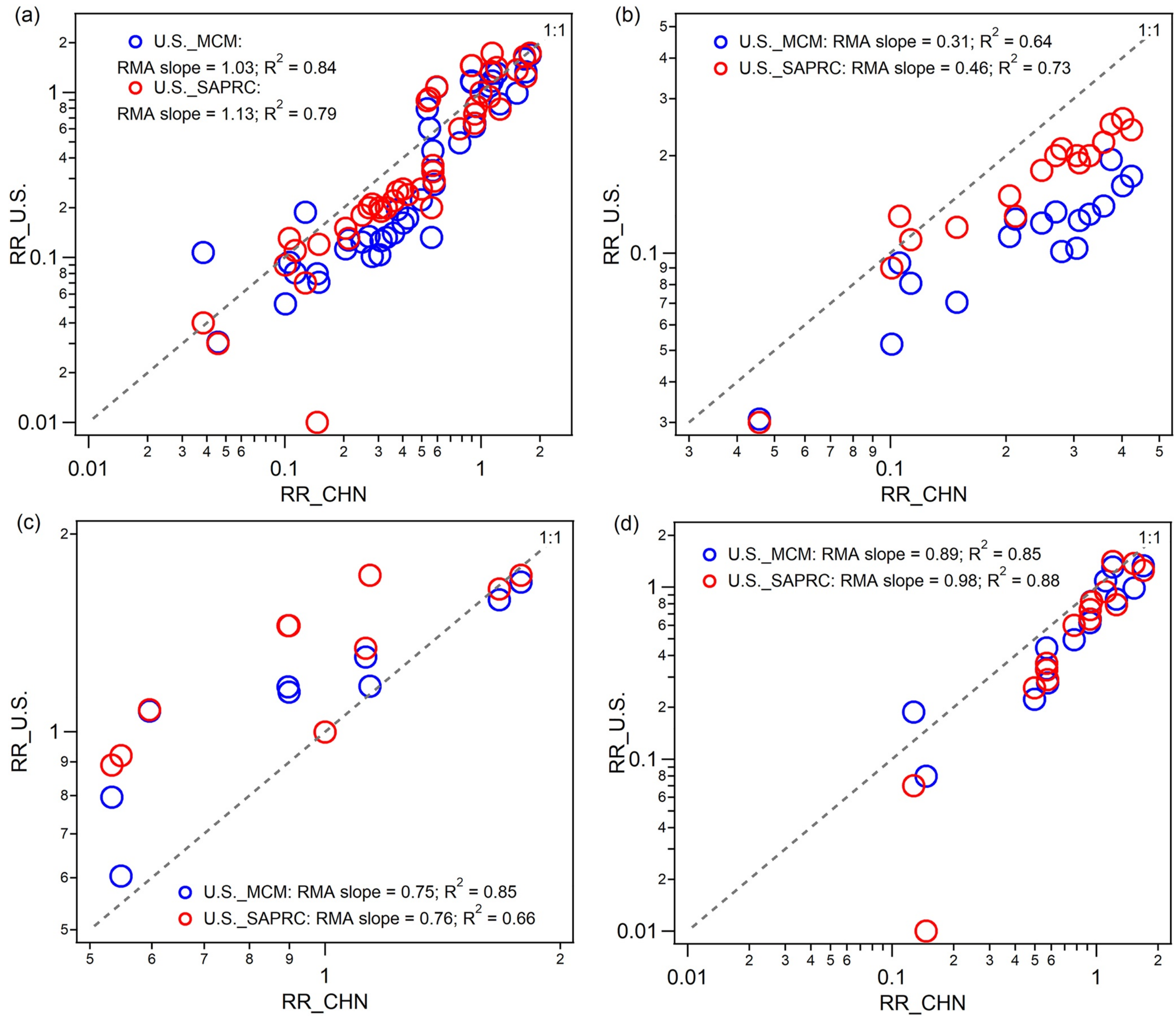

Figure 4. Comparison of the RRs (calculated as the MIR values for a given species divided by the MIR value for ethene) for (a) 44 common VOC species, (b) alkanes, (c) alkenes, and (d) aromatics between Averaged Chinese (RR_CHN) and U.S. (US_MCM in blue circle and US_SAPRC in red circle) Urban Condition Scenario. The RRs for VOCs in U.S. were obtained from Carter (2010) and Derwent et al. (2010).

(10 species; including both anthropogenic and biogenic species), and aromatics (15 species)), and found that the improvement mainly resulted from alkenes (R^2: CHN_MCM vs. US_MCM: 0.85; CHN_MCM vs. US_SAPRC: 0.66). This conclusion is also supported by the comparison between US_SAPRC and US_MCM, as RRs for alkenes showed the lowest correlation between two chemical mechanisms (R^2 for alkenes: 0.71; alkanes: 0.81; aromatics: 0.92), but the detailed reason remains unclear (Derwent et al., 2010).

We then compared the magnitudes for RRs between CHN_MCM and US_SAPRC/MCM based on RMA slope, which showed insignificant variations for the 44 species (US_SAPRC: higher by 13% than CHN-MCM, $p = 0.96$; US_MCM: higher by 3% than CHN-MCM, $p = 0.59$). Specific to individual major VOCs groups, the RR magnitudes for alkanes, alkenes, and aromatics were all higher in China than in U.S., both with the same (MCM v3.3.1 vs. MCM v3.1; by 69% ($p < 0.01$), 25% ($p = 0.44$), and 11% ($p = 0.19$), respectively) and different chemical mechanisms (MCM v3.3.1 vs. SAPRC07; 54% ($p = 0.07$), 24% ($p = 0.09$), and 2% ($p = 0.24$), respectively). The inconsistency can be explained by the large intercept for alkenes obtained from the linear regression analysis (Figure 4c), and hence, we focused on the variations of total VOCs, alkanes, and aromatics in the following

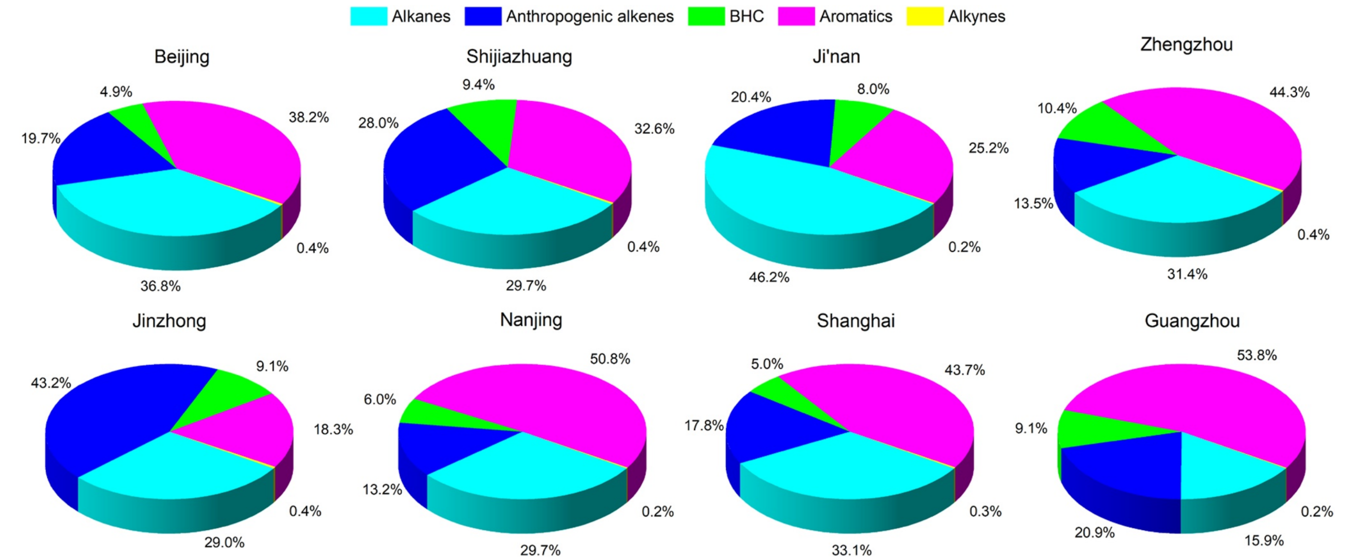

Figure 5. The contributions of major VOCs groups (i.e., alkanes, anthropogenic alkenes, BHC, aromatics, and alkynes) to total Conw_OFPs for 57 PAMS species in eight major cities of Central-Eastern China. The Conw_OFPs were quantified using averages of observation data during 6:00–7:00 LT for anthropogenic VOCs and during 12:00–14:00 LT for biogenic VOCs.

analyses. The discrepancy in RR magnitudes still existed with the same chemical mechanism, thereby implying the influence of other factors in addition to chemical mechanism. A further inspection revealed the remarkable difference in chemical environmental conditions between China and the U.S. (a lower VOCs/NO_x ratio (4.9 vs. 6.5) and higher contribution of alkanes (66% vs. 52%) in China), which would certainly exert effects on RR magnitudes as demonstrated by our previous study (Zhang et al., 2021). For instance, one-fourth of the base VOCs/NO_x ratios tended to decrease the RR magnitudes for total VOCs (−9%), but would increase the RRs for alkanes (4%) and aromatics (2%); 1.5-fold of the base proportion of the alkane class would increase the RR magnitudes for total VOCs (15%), alkanes (6%), and aromatics (7%). The discrepancy in RR magnitudes between China and the U.S. should be a complex coupling of these factors.

3.4. Implications for VOCs Management

The localized MIRs were used to quantify Conw_OFPs and identify key VOCs group (Figure 5). The exact key VOCs group varied among cities. In the BTHs region, alkanes and aromatics were key groups in Ji'nan (46%) and Zhengzhou (44%), respectively, while these two groups made comparable contributions in Beijing (37% and 38%) and Shijiazhuang (30% and 33%). The dominant role of alkanes to O_3 formation in Ji'nan was attributed to its high contributions of alkane species (76% vs. 59%–71% in other cities; see Figure 2), especially of C_3–C_5 alkane species. In the FWP region, anthropogenic alkenes were the dominant group with an average contribution of 43%. In the YRD and PRD regions, aromatics were key group with average contributions of 51%, 44%, and 54% in Nanjing, Shanghai, and Guangzhou, respectively. Though the concentrations of BHC made small contributions (1%–2%) to total VOCs, they made a non-negligible contribution to O_3 formation (5%–10%) based on Conw_OFPs. Notably, the key VOCs groups identified based on L_{OH} (see Figure 2b) and Conw_OFPs are not that consistent, as L_{OH} only considers the first step of VOCs oxidation (i.e., reactions with OH radicals) and ignores the contributions from its chemical degradation intermediates and products. Overall, the Conw_OFPs results highlight the importance of aromatics to O_3 formation in the vast Chinese urban areas, and its importance increased toward lower latitudes, which is consistent with findings from previous studies (Wang et al., 2022).

Figure 6 presents the top 10 VOC species with relatively large Conw_OFPs over individual cities. These 10 species made important contributions (62%–79%) to the summed Conw_OFPs for total 57 PAMS species, and reduction in emissions for these species would effectively alleviate O_3 pollution. Lists for the top 10 species varied among cities, but ethene, isoprene, toluene, *n*-butane, *i*-pentane, and *m*-xylene were found to make important contributions to O_3 formation in most cities. Though species such as propane were relatively unreactive (i.e., with a low MIR value), their importance could be enhanced by heavy loads of emissions (see Figure 6 for the

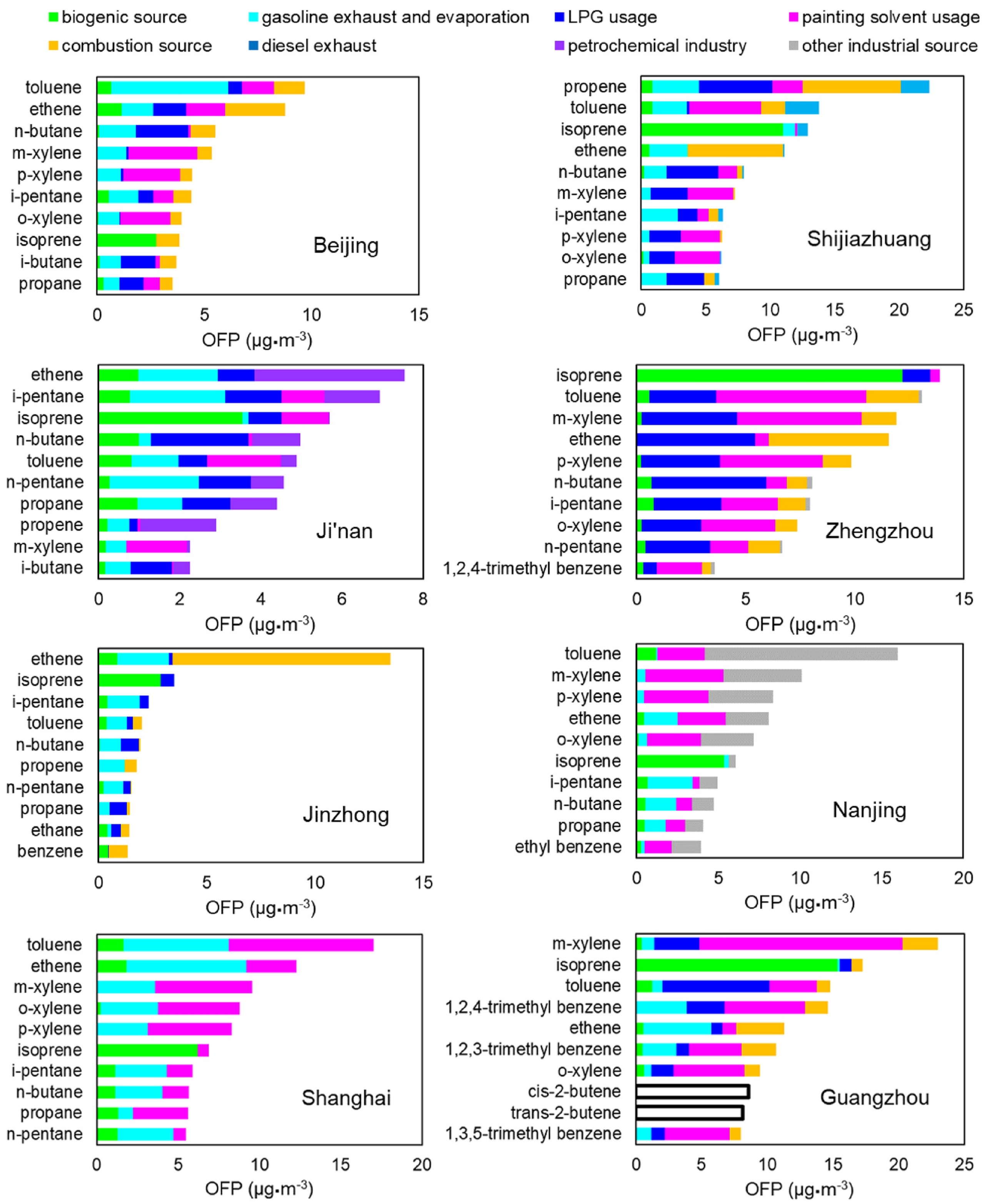

Figure 6. Source-specific contributions to the individual top 10 VOC species with large Conw_OFPs in eight major cities of Central-Eastern China. The Conw_OFPs were determined with the application of localized MIRs. The data caption rates of *cis*/*trans*-2-butene in Guangzhou were below 75% and hence excluded for source apportionment analyses.

Conw_OFPs in Beijing, Shijiazhuang, Ji'nan, Jinzhong, Nanjing, and Shanghai). Both chemical reactivity and mass/concentration for VOCs species should be considered in the formulation of control policy against VOCs and O_3 pollution.

Sources for these key species were quantitatively tracked using the positive matrix factorization (PMF) model (Figure 6 and Figure S7 in Supporting Information S2; Paatero, 1997; Paatero & Tapper, 1994). Detailed information about the PMF model setup, factor contributions and factor profiles of VOCs were provided in the SI. Here we focused on the source-specific contributions to the Conw_OFPs for these species. Two important points are noteworthy. First, the dominant sources varied largely among individual cities. In the BTHs region, gasoline exhaust and evaporation and painting solvent usage were dominant contributors to the summed Conw_OFPs for key species in Beijing (29% and 26%, respectively); petrochemical industry and gasoline exhaust and evaporation made dominant contributions in Ji'nan (24% and 23%); while LPG usage and painting solvent usage were dominant contributors in Shijiazhuang (21% and 21%) and Zhengzhou (35% and 31%). In the FWP region, combustion source made the largest contribution (41%) in Jinzhong. In the YRD region, industrial activity made the largest contribution in Nanjing (44%), while painting solvent usage and gasoline exhaust and evaporation made dominant contributions in Shanghai (42% and 40%). In the PRD region, painting solvent usage made the largest contribution (37%) in Guangzhou. The above-identified dominant VOCs sources were generally consistent with those reported in previous studies (Liu et al., 2019; Lyu et al., 2019; Yang et al., 2021; Zhao et al., 2020). Second, the dominant VOCs sources identified based on concentrations and Conw_OFPs are not that consistent. For example, the concentration-based results indicate that LPG usage made the largest contribution in Beijing, while that is gasoline exhaust and evaporation with the OFP-based results. Similar conclusion was also drawn by Zhao et al. (2020) in which diesel vehicular exhaust and industrial emission were identified as the dominant VOCs sources in Nanjing with concentration-based and OFP-based results, respectively. These results underline the importance of city-specific refined VOCs emission control strategies.

The key VOC species and source contributions determined based upon localized MIRs and the extensively used U.S. MIRs were compared to examine to what extent the ongoing air quality management strategies would change. Lists for the top 10 species remain unchanged in Ji'nan, but varied (with 1–2 species changed) in other cities (labeled in Figure S8 in Supporting Information S2). With the application of U.S. MIRs, the importance of alkenes (especially propene) was enhanced, but that of alkanes was reduced. Correspondingly, the contributions of combustion source (characterized by high concentration levels of acetylene, benzene, and/or ethene and propene) became larger (by 0%–4%), but of gasoline exhaust and evaporation (characterized by high concentration levels of *n*/*i*-pentane and/or toluene and ethyl benzene) were lowered (by −4% to 0%). In particular, LPG usage (localized MIRs: 21% vs. U.S. MIRs: 19%) and painting solvent usage (21% vs. 19%) were replaced by combustion source (19% vs. 22%) to be the dominant contributor in Shijiazhuang; petrochemical industry (24% vs. 25%) alone (rather than with gasoline exhaust and evaporation: 23% vs. 20%) was identified as the dominant contributor in Ji'nan. These results indicate that the application of U.S. MIRs would lead to uncertainties in the identification of key VOC species and major sources, and thus highlight the necessity of MIR localization.

The MIR scales are suitable for application for areas or episodes in VOCs-limited O_3 formation regime, which is the case for a large variety of urban areas over China in the current stage. Previous studies found an spatial expansion in mixed-limited O_3 formation regime, owing to decreasing NO_x and increasing (or at least non-decreasing) VOCs emission in recent years (Jin & Holloway, 2015). In consideration of the high dependence of IR values on NO_x condition (Zhang et al., 2021), we need to regularly update the applied IR scales based on changes in NO_x condition in the future.

4. Conclusions

The localized MIRs for 57 PAMS VOC species were developed in eight major cities over Central-Eastern China, with application of the MCM box model coupled with comprehensive observation inputs. The observations reveal a serious O_3 pollution situation in China, particularly in the BTHs. Though differ largely in chemical environments (such as the concentration of VOCs and NO_x, VOCs/NO_x ratio, and VOCs composition), all of the cities are in VOCs-limited O_3 formation regime, and thus the MIR scales are appropriate for application. The localized MIRs are highly consistent among individual cities and well agreed with the regional representative average MIRs (except for Guangzhou), which indicates that the regional average MIR scales could serve as a general scale to approximate reactivities in urban areas without significant changes in atmospheric conditions.

Despite a same overall pattern, the localized MIRs differed from those obtained based on the U.S. urban conditions with respect to a few compounds, owing to a combined influence of chemical mechanisms and chemical environmental conditions. The localized MIRs were applied to quantify the Conw_OFPs. Ethene, isoprene, toluene, *n*-butane, *i*-pentane, and *m*-xylene were identified as key species over Chinese urban areas, the control of which would effectively alleviate local O_3 formation. The source-specific contributions to the Conw_OFPs for top 10 key species showed large variance among cities, underlining the importance of city-specific refined VOCs emission reduction measures. This study fills the gap of localized MIRs for VOCs in urban areas of China, and the findings provide important references for the formulation of control strategies against VOCs and O_3 pollution.

Data Availability Statement

The code for the MCM chemical box model can be downloaded from Zenodo (https://doi.org/10.5281/zenodo.5752566 (Wolfe & Haskins, 2021) [Software]). Data associated with this paper are accessible at Mendeley Data (https://doi.org/10.17632/g76knbxjxn.1 (Zhang & Xue, 2022) [Dataset]).

Acknowledgments

We thank William Carter and Richard Derwent for providing the MIR data of the California scenarios, Glenn Wolfe for providing the platform of F0AM, the University of York for providing the Master Chemical Mechanism (version 3.3.1), and the local Environmental Protection Agencies for the provision of field observation data. This work was sponsored by the National Natural Science Foundation of China (41922051), the Shandong Provincial Science Foundation for Distinguished Young Scholars (ZR2019JQ09), and the Jiangsu Collaborative Innovation Center for Climate Change.

References

Atkinson, R., & Arey, J. (2003). Atmospheric degradation of volatile organic compounds. *Chemical Reviews*, *103*(12), 4605–4638. https://doi.org/10.1021/cr0206420

Carter, W. (1994a). Calculation of reactivity scales using an updated carbon bond IV mechanism, report prepared for systems applications international for the auto/oil air quality improvement program.

Carter, W. (1994b). Development of ozone reactivity scales for volatile organic compounds. *Journal of the Air & Waste Management Association*, *44*(7), 881–899. https://doi.org/10.1080/1073161X.1994.10467290

Carter, W. (2009). *Updated maximum incremental reactivity scale and hydrocarbon bin reactivities for regulatory applications*. California Air Resources Board Contract.

Carter, W. (2010). Development of the SAPRC-07 chemical mechanism. *Atmospheric Environment*, *44*(40), 5324–5335. https://doi.org/10.1016/j.atmosenv.2010.01.026

Chang, T., & Rudy, S. (1990). Ozone-forming potential of organic emissions from alternative-fueled vehicles. *Atmospheric Environment*, *24*(9), 2421–2430. https://doi.org/10.1016/0960-1686(90)90335-K

Chen, T., Xue, L., Zheng, P., Zhang, Y., Liu, Y., Sun, J., et al. (2020). Volatile organic compounds and ozone air pollution in an oil production region in Northern China. *Atmospheric Chemistry and Physics*, *20*(11), 7069–7086. https://doi.org/10.5194/acp-20-7069-2020

CNEMC. (2018). Technical specifications for operations and quality control of ambient air quality continuous automated monitoring system for SO_2, NO_2, O_3 and CO (in Chinese). Retrieved from http://www.cnemc.cn/jcgf/dqhj/202009/W020200922483880824988.pdf

CNEMC. (2019). Technical specifications for operation and quality control of ambient air quality continuous automated monitoring system for volatile organic compounds (trial) (in Chinese). Retrieved from http://www.cnemc.cn/gzdt/wjtz/202001/W020200101619478251660.pdf

Derwent, R., Jenkin, M., Pilling, M., Carter, W., & Kaduwela, A. (2010). Reactivity scales as comparative tools for chemical mechanisms. *Journal of the Air & Waste Management Association*, *60*(8), 914–924. https://doi.org/10.3155/1047-3289.60.8.914

Fleming, Z., Doherty, R., Schneidemesser, E., Malley, C., Cooper, O., Pinto, J., et al. (2018). Tropospheric Ozone Assessment Report: Present-day ozone distribution and trends relevant to human health. *Elementa: Science of the Anthropocene*, *6*. https://doi.org/10.1525/elementa.273

Gu, R., Shen, H., Xue, L., Wang, T., Gao, J., Li, H., et al. (2022). Investigating the sources of atmospheric nitrous acid (HONO) in the megacity of Beijing, China. *Science of the Total Environment*, *812*, 152270. https://doi.org/10.1016/j.scitotenv.2021.152270

Gu, R., Zheng, P., Chen, T., Dong, C., Wang, Y., Liu, Y., et al. (2020). Atmospheric nitrous acid (HONO) at a rural coastal site in North China: Seasonal variations and effects of biomass burning. *Atmospheric Environment*, *229*, 117429. https://doi.org/10.1016/j.atmosenv.2020.117429

Guo, H., Ling, Z., Cheng, H., Simpson, I., Lyu, X., Wang, X., et al. (2017). Tropospheric volatile organic compounds in China. *Science of the Total Environment*, *574*, 1021–1043. https://doi.org/10.1016/j.scitotenv.2016.09.116

Jenkin, M., Derwent, R., & Wallington, T. (2017). Photochemical ozone creation potentials for volatile organic compounds: Rationalization and estimation. *Atmospheric Environment*, *163*, 128–137. https://doi.org/10.1016/j.atmosenv.2017.05.024

Jenkin, M., Saunders, S., Wagner, V., & Pilling, M. (2003). Protocol for the development of the master chemical mechanism, MCM v3 (Part B): Tropospheric degradation of aromatic volatile organic compounds. *Atmospheric Chemistry and Physics*, *3*(1), 181–193. https://doi.org/10.5194/acp-3-181-2003

Jenkin, M., Valorso, R., Aumont, B., Rickard, A., & Wallington, T. (2018a). Estimation of rate coefficients and branching ratios for gas-phase reactions of OH with aliphatic organic compounds for use in automated mechanism construction. *Atmospheric Chemistry and Physics*, *18*(13), 9297–9328. https://doi.org/10.5194/acp-18-9297-2018

Jenkin, M., Valorso, R., Aumont, B., Rickard, A., & Wallington, T. (2018b). Estimation of rate coefficients and branching ratios for gas-phase reactions of OH with aromatic organic compounds for use in automated mechanism construction. *Atmospheric Chemistry and Physics*, *18*(13), 9329–9349. https://doi.org/10.5194/acp-18-9329-2018

Jenkin, M., Young, J., & Rickard, A. (2015). The MCM v3.3.1 degradation scheme for isoprene. *Atmospheric Chemistry and Physics*, *15*(20), 11433–11459. https://doi.org/10.5194/acp-15-11433-2015

Jin, X., & Holloway, T. (2015). Spatial and temporal variability of ozone sensitivity over China observed from the Ozone Monitoring Instrument. *Journal of Geophysical Research: Atmospheres*, *120*(14), 7229–7246. https://doi.org/10.1002/2015JD023250

Leduc, D. (1987). A comparative analysis of the reduced major axis technique of fitting lines to bivariate data. *Canadian Journal of Forest Research*, *17*(7), 654–659. https://doi.org/10.1139/x87-107

Li, M., Zhang, Q., Kurokawa, J., Woo, J., He, K., Lu, Z., et al. (2017). Mix: A mosaic Asian anthropogenic emission inventory under the international collaboration framework of the MICS-Asia and HTAP. *Atmospheric Chemistry and Physics*, *17*(2), 935–963. https://doi.org/10.5194/acp-17-935-2017

Li, M., Zhang, Q., Zheng, B., Tong, D., Lei, Y., Liu, F., et al. (2019). Persistent growth of anthropogenic non-methane volatile organic compound (NMVOC) emissions in China during 1990–2017: Drivers, speciation and ozone formation potential. *Atmospheric Chemistry and Physics*, *19*(13), 8897–8913. https://doi.org/10.5194/acp-19-8897-2019

Liu, Y., Wang, H., Jing, S., Gao, Y., Peng, Y., Lou, S., et al. (2019). Characteristics and sources of volatile organic compounds (VOCs) in Shanghai during summer: Implications of regional transport. *Atmospheric Environment*, *215*, 116902. https://doi.org/10.1016/j.atmosenv.2019.116902

Liu, Y., & Wang, T. (2020a). Worsening urban ozone pollution in China from 2013 to 2017 – Part 1: The complex and varying roles of meteorology. *Atmospheric Chemistry and Physics*, *20*(11), 6305–6321. https://doi.org/10.5194/acp-20-6305-2020

Liu, Y., & Wang, T. (2020b). Worsening urban ozone pollution in China from 2013 to 2017 – Part 2: The effects of emission changes and implications for multi-pollutant control. *Atmospheric Chemistry and Physics*, *20*(11), 6323–6337. https://doi.org/10.5194/acp-20-6323-2020

Lu, H., Lyu, X., Cheng, H., Ling, Z., & Guo, H. (2019). Overview on the spatial–temporal characteristics of the ozone formation regime in China. *Environmental Science: Processes & Impacts*, *21*(6), 916–929. https://doi.org/10.1039/C9EM00098D

Lu, X., Hong, J., Zhang, L., Cooper, O., Schultz, M., Xu, X., et al. (2018). Severe surface ozone pollution in China: A global perspective. *Environmental Science and Technology Letters*, *5*(8), 487–494. https://doi.org/10.1021/acs.estlett.8b00366

Lyu, X., Wang, N., Guo, H., Xue, L., Jiang, F., Zeren, Y., et al. (2019). Causes of a continuous summertime O_3 pollution event in Jinan, a central city in the North China Plain. *Atmospheric Chemistry and Physics*, *19*(5), 3025–3042. https://doi.org/10.5194/acp-19-3025-2019

McGillen, M., Carter, W., Mellouki, A., Orlando, J., Picquet-Varrault, B., & Wallington, T. (2020). Database for the kinetics of the gas-phase atmospheric reactions of organic compounds. *Earth System Science Data*, *12*(2), 1203–1216. https://doi.org/10.5194/essd-12-1203-2020

Mo, Z., Huang, S., Yuan, B., Pei, C., Song, Q., Qi, J., et al. (2020). Deriving emission fluxes of volatile organic compounds from tower observation in the Pearl River Delta, China. *Science of the Total Environment*, *741*, 139763–139771. https://doi.org/10.1016/j.scitotenv.2020.139763

Mo, Z., Huang, S., Yuan, B., Pei, C., Song, Q., Qi, J., et al. (2022). Tower-based measurements of NMHCs and OVOCs in the Pearl River Delta: Vertical distribution, source analysis and chemical reactivity. *Environmental Pollution*, *292*, 118454. https://doi.org/10.1016/j.envpol.2021.118454

NRC. (1999). *Ozone-Forming potential of reformulated gasoline*. The National Academies Press. https://doi.org/10.17226/9461

Paatero, P. (1997). Least squares formulation of robust non-negative factor analysis. *Chemometrics and Intelligent Laboratory Systems*, *37*(1), 23–35. https://doi.org/10.1016/S0169-7439(96)00044-5

Paatero, P., & Tapper, U. (1994). Positive matrix factorization: A non-negative factor model with optimal utilization of error estimates of data values. *Environmetrics*, *5*(2), 111–126. https://doi.org/10.1002/env.3170050203

Pei, C., Yang, W., Zhang, Y., Song, W., Xiao, S., Wang, J., et al. (2022). Decrease in ambient volatile organic compounds during the COVID-19 lockdown period in the Pearl River Delta region, south China. *Science of The Total Environment*, *823*, 153720. https://doi.org/10.1016/j.scitotenv.2022.153720

Qiu, W., Liu, Y., Tan, Z., Chen, X., Lu, K., & Zhang, Y. (2020). Calculation of maximum incremental reactivity scales based on typical megacities in China. *Chinese Science Bulletin*, *65*(7), 610–621. https://doi.org/10.1360/tb-2019-0598

Russell, A., Milford, J., Bergin, M., Mcbride, S., Mcnair, L., Yang, Y., et al. (1995). Urban ozone control and atmospheric reactivity of organic gases. *Science*, *269*(5223), 491–495. https://doi.org/10.1126/science.269.5223.491

Saunders, S., Jenkin, M., Derwent, R., & Pilling, M. (2003). Protocol for the development of the master chemical mechanism, MCM v3 (Part A): Tropospheric degradation of non-aromatic volatile organic compounds. *Atmospheric Chemistry and Physics*, *3*(1), 161–180. https://doi.org/10.5194/acp-3-161-2003

Sha, Q., Zhu, M., Huang, H., Wang, Y., Huang, Z., Zhang, X., et al. (2021). A newly integrated dataset of volatile organic compounds (VOCs) source profiles and implications for the future development of VOCs profiles in China. *Science of the Total Environment*, *793*, 148348. https://doi.org/10.1016/j.scitotenv.2021.148348

Shi, Y., Liu, C., Zhang, B., Simayi, M., Xi, Z., Ren, J., & Xie, S. (2022). Accurate identification of key VOCs sources contributing to O_3 formation along the Liaodong Bay based on emission inventories and ambient observations. *Science of the Total Environment*, *844*, 156998. https://doi.org/10.1016/j.scitotenv.2022.156998

Solomon, P., Vallano, D., Lunden, M., LaFranchi, B., Blanchard, C., & Shaw, S. (2020). Mobile-platform measurement of air pollutant concentrations in California: Performance assessment, statistical methods for evaluating spatial variations, and spatial representativeness. *Atmospheric Measurement Techniques*, *13*(6), 3277–3301. https://doi.org/10.5194/amt-13-3277-2020

Sun, L., Xue, L., Wang, T., Gao, J., Ding, A., Cooper, O., et al. (2016). Significant increase of summertime ozone at Mount Tai in Central Eastern China. *Atmospheric Chemistry and Physics*, *16*(16), 10637–10650. https://doi.org/10.5194/acp-16-10637-2016

Venecek, M., Carter, W., & Kleeman, M. (2018). Updating the SAPRC maximum incremental reactivity (MIR) scale for the United States from 1988 to 2010. *Journal of the Air & Waste Management Association*, *68*(12), 1301–1316. https://doi.org/10.1080/10962247.2018.1498410

Wang, T., Dai, J., Lam, K., Poon, C., & Brasseur, G. (2019). Twenty-five years of lower tropospheric ozone observations in tropical East Asia: The influence of emissions and weather patterns. *Geophysical Research Letters*, *46*(20), 11463–11470. https://doi.org/10.1029/2019gl084459

Wang, T., Xue, L., Brimblecombe, P., Lam, Y., Li, L., & Zhang, L. (2017). Ozone pollution in China: A review of concentrations, meteorological influences, chemical precursors, and effects. *Science of The Total Environment*, *575*, 1582–1596. https://doi.org/10.1016/j.scitotenv.2016.10.081

Wang, T., Xue, L., Feng, Z., Dai, J., Zhang, Y., & Tan, Y. (2022). Ground-level ozone pollution in China: A synthesis of recent findings on influencing factors and impacts. *Environmental Research Letters*, *17*(6), 063003. https://doi.org/10.1088/1748-9326/ac69fe

Wolfe, G., & Haskins, J. (2021). AirChem/F0AM v4.2.1 [Software]. Zenodo. https://doi.org/10.5281/zenodo.5752566

Wolfe, G., Marvin, M., Roberts, S., Travis, K., & Liao, J. (2016). The framework for 0-D atmospheric modeling (F0AM) v3.1. *Geoscientific Model Development*, *9*(9), 3309–3319. https://doi.org/10.5194/gmd-9-3309-2016

Xu, X. (2021). Recent advances in studies of ozone pollution and impacts in China: A short review. *Current Opinion in Environmental Science & Health*, *19*, 100225–100234. https://doi.org/10.1016/j.coesh.2020.100225

Xu, X., Lin, W., Xu, W., Jin, J., Wang, Y., Zhang, G., et al. (2020). Long-term changes of regional ozone in China: Implications for human health and ecosystem impacts. *Elementa: Science of the Anthropocene*, *8*, 13. https://doi.org/10.1525/elementa.409

Xue, L., Wang, T., Gao, J., Ding, A. J., Zhou, X., Blake, D., et al. (2014). Ground-level ozone in four Chinese cities: Precursors, regional transport and heterogeneous processes. *Atmospheric Chemistry and Physics*, *14*(23), 13175–13188. https://doi.org/10.5194/acp-14-13175-2014

Xue, L., Wang, T., Guo, H., Blake, D., Tang, J., Zhang, X., et al. (2013). Sources and photochemistry of volatile organic compounds in the remote atmosphere of Western China: Results from the Mt. Waliguan observatory. *Atmospheric Chemistry and Physics*, *13*(17), 8551–8567. https://doi.org/10.5194/acp-13-8551-2013

Yang, S., Li, X., Song, M., Liu, Y., Yu, X., Chen, S., et al. (2021). Characteristics and sources of volatile organic compounds during pollution episodes and clean periods in the Beijing-Tianjin-Hebei region. *Science of the Total Environment*, *799*, 149491. https://doi.org/10.1016/j.scitotenv.2021.149491

Zhang, C., Song, Y., Wang, H., Zeng, L., Hu, M., Lu, K., et al. (2022). Observation-Based estimations of relative ozone impacts by using volatile organic compounds reactivities. *Environmental Science and Technology Letters*, *9*(1), 10–15. https://doi.org/10.1021/acs.estlett.1c00835

Zhang, Y., & Xue, L. (2022). Observational data in 8 representative cities of Central-Eastern China (Version 1) [Dataset]. Mendeley Data. https://data.mendeley.com/datasets/g76knbxjxn/1

Zhang, Y., Xue, L., Carter, W., Pei, C., Chen, T., Mu, J., et al. (2021). Development of ozone reactivity scales for volatile organic compounds in a Chinese megacity. *Atmospheric Chemistry and Physics*, *21*(14), 11053–11068. https://doi.org/10.5194/acp-21-11053-2021

Zhao, Q., Bi, J., Liu, Q., Ling, Z., Shen, G., Chen, F., et al. (2020). Sources of volatile organic compounds and policy implications for regional ozone pollution control in an urban location of Nanjing, East China. *Atmospheric Chemistry and Physics*, *20*(6), 3905–3919. https://doi.org/10.5194/acp-20-3905-2020

Zheng, B., Tong, D., Li, M., Liu, F., Hong, C., Geng, G., et al. (2018). Trends in China's anthropogenic emissions since 2010 as the consequence of clean air actions. *Atmospheric Chemistry and Physics*, *18*(19), 14095–14111. https://doi.org/10.5194/acp-18-14095-2018

References From the Supporting Information

Li, J., Wu, R., Li, Y., Hao, Y., Xie, S., & Zeng, L. (2016). Effects of rigorous emission controls on reducing ambient volatile organic compounds in Beijing, China. *Science of The Total Environment*, *557–558*, 531–541. https://doi.org/10.1016/j.scitotenv.2016.03.140

Li, Z., Ho, K., & Yim, S. (2020). Source apportionment of hourly-resolved ambient volatile organic compounds: Influence of temporal resolution. *Science of The Total Environment*, *725*, 138243. https://doi.org/10.1016/j.scitotenv.2020.138243